

# Probe of extra dimensions in $\gamma q \rightarrow \gamma q$ at the LHC

İ. Şahin,<sup>1,\*</sup> A. A. Billur,<sup>2,†</sup> S. C. İnan,<sup>2,‡</sup> B. Şahin,<sup>1,§</sup>

M. Köksal,<sup>2,¶</sup> P. Tektaş,<sup>1</sup> E. Alıcı,<sup>1</sup> and R. Yıldırım<sup>2</sup>

<sup>1</sup>*Department of Physics, Bulent Ecevit University, 67100 Zonguldak, Turkey*

<sup>2</sup>*Department of Physics, Cumhuriyet University, 58140 Sivas, Turkey*

## Abstract

We have examined TeV scale effects of extra spatial dimensions through the processes  $\gamma q \rightarrow \gamma q$  where  $q = u, d, c, s, b, \bar{u}, \bar{d}, \bar{c}, \bar{s}, \bar{b}$ . These processes have been treated in a photon-proton collision via the main reaction  $pp \rightarrow p\gamma p \rightarrow p\gamma qX$  at the LHC. We have employed equivalent photon approximation for incoming photon beams and performed statistical analysis for various forward detector acceptances.

---

\*inancsahin@karaelmas.edu.tr

†abillur@cumhuriyet.edu.tr

‡sceminan@cumhuriyet.edu.tr

§bsahin@karaelmas.edu.tr

¶mkoksal@cumhuriyet.edu.tr

## I. INTRODUCTION

Extra spatial dimensions that show themselves near the TeV scale have been widely studied in particle physics since the pioneering works of Arkani-Hamed, Dimopoulos and Dvali (ADD) [1–3]. Soon after the work of ADD a warped model was proposed by Randall and Sundrum (RS) [4]. According to ADD and RS models, extra spatial dimensions can have observable effects at the TeV scale physics. The possibility of these extra dimensions has been probed in the past colliders but no evidence has been found. The Large Hadron Collider (LHC) offers the opportunity of a very rich physics program. Signals confirming the existence of extra dimensions might become detectable in the high energetic collisions of the LHC. Phenomenological studies on extra dimensions involving quark-quark, gluon-gluon or quark-gluon collisions at the LHC are widespread in the literature. On the other hand, extra dimensions have been much less studied in photon-induced reactions ( $\gamma\gamma$  or  $\gamma$ -proton collisions) at the LHC.

In an usual proton-proton deep inelastic scattering (DIS) processes both of the incoming protons dissociate into partons. Due to proton remnants, usual DIS processes do not provide a clean environment. Jets coming from proton remnants create some uncertainties and make it difficult to discern the signals which may arise from the new physics beyond the standard model. On the other hand, in  $\gamma\gamma$  or  $\gamma$ -proton collisions with quasireal photons, photon emitting protons remains intact.  $\gamma\gamma$  processes provide the most clean channels due to absence of the remnants of both proton beams. Whereas in  $\gamma$ -proton processes one of the incoming protons dissociate into partons but other proton remains intact. Midway from proton-proton DIS to  $\gamma\gamma$ ,  $\gamma$ -proton processes have less experimental uncertainties compared with proton-proton processes. Furthermore, they have higher energy reach and effective luminosity with respect to  $\gamma\gamma$  processes [5–7].

In this work we have investigated TeV scale effects of extra spatial dimensions via the process  $\gamma q \rightarrow \gamma q$  at the LHC. The process  $\gamma q \rightarrow \gamma q$  takes part as a subprocess in the main reaction  $pp \rightarrow p\gamma p \rightarrow p\gamma q X$  (Fig.1). The photon which enters the subprocess is emitted from one of the proton beams and described by equivalent photon approximation (EPA) [8–10]. In the framework of EPA, virtuality of the quasireal photons is very low. Hence when a proton emits a quasireal photon, it does not dissociate into partons. In EPA, quasireal photons carry a small transverse momentum. Therefore photon emitting intact protons

deviate slightly from their trajectory along the beam path. They are generally scattered with very small angles from the beam pipe and exit the central detector without being detected. Consequently, detection of intact protons needs forward detector equipment in addition to central detectors. It is foreseen to equip ATLAS and CMS central detectors with very forward detectors which can detect intact scattered protons with a very large pseudorapidity. A project called AFP (ATLAS Forward Physics) that aims to install very forward detectors located at distances 220 and 420 m from the interaction point, is under evaluation in the ATLAS collaboration [11, 12]. The acceptance proposed by AFP project is  $0.0015 < \xi < 0.15$  where  $\xi$  is the momentum fraction loss of the intact scattered protons. Mathematically speaking, it is defined by the formula  $\xi = (|\vec{p}| - |\vec{p}'|)/|\vec{p}|$ . Here  $\vec{p}$  is the momentum of incoming proton and  $\vec{p}'$  is the momentum of intact scattered proton. At the LHC energies, it is a good approximation to write  $\xi = \frac{E_\gamma}{E}$  where  $E_\gamma$  is the energy of the emitted quasireal photon and  $E$  is the energy of the incoming proton. There are also other scenarios with different acceptances. When forward detectors are placed closer to the interaction point they can detect protons with higher  $\xi$ . In the CMS-TOTEM forward detector scenario, a forward detector acceptance of  $0.0015 < \xi < 0.5$  is considered [13, 14]. This wide acceptance range is provided by the use of the detectors of TOTEM experiment at 147 and 220 m from the CMS interaction point in addition to forward detectors at 420 m.

Existence of photon-induced reactions in a hadron collider is not merely a theoretical hypothesis. Photon-induced reactions in a hadron-hadron collision were verified experimentally at the Fermilab Tevatron [15–17]. The reactions such as  $p\bar{p} \rightarrow p\gamma\gamma\bar{p} \rightarrow pe^+e^-\bar{p}$  [15, 16],  $p\bar{p} \rightarrow p\gamma\gamma\bar{p} \rightarrow p\mu^+\mu^-\bar{p}$  [16, 17],  $p\bar{p} \rightarrow p\gamma\bar{p} \rightarrow pJ/\psi(\psi(2S))\bar{p}$  [17] were observed by the CDF collaboration. From the early LHC data obtained in proton-proton collisions at  $\sqrt{s} = 7$  TeV, two-photon reactions  $pp \rightarrow p\gamma\gamma p \rightarrow p\mu^+\mu^-p$  and  $pp \rightarrow p\gamma\gamma p \rightarrow pe^+e^-p$  have been observed by the CMS Collaboration [18, 19]. Probing new physics via photon-photon and photon-proton reactions at the LHC has been studied in the literature. Phenomenological studies cover a wide range of new physics such as supersymmetry, extra dimensions, unparticle physics, anomalous interaction of standard model particles, magnetic monopoles, etc. [6, 14, 20–46].

## II. ADD MODEL OF LARGE EXTRA DIMENSIONS

ADD model was proposed as a solution to the hierarchy problem which is known as the unexplained large difference between the electroweak scale  $\sim \mathcal{O}(100 \text{ GeV})$  and the Planck scale  $M_{Pl} \sim \mathcal{O}(10^{19} \text{ GeV})$  [1–3]. According to ADD model, gravity can propagate in a  $4 + \delta$  dimensional space called "bulk" but Standard Model (SM) particles are confined in a hypersurface called "brane". Using Gauss' law in arbitrary dimensions, 4-dimensional Planck scale can be related to the  $(4 + \delta)$ -dimensional fundamental scale  $M_D$  through the formula

$$M_{Pl}^2 = 8\pi R^\delta M_D^{2+\delta}. \quad (1)$$

Here,  $R$  is the radius of the compactified extra dimensional space of dimension  $\delta$  and volume  $V_\delta = (2\pi R)^\delta$ . In the ADD model, the hierarchy is eliminated by choosing the compactification radius large. For instance if we choose  $R \sim 0.1 \text{ mm}$  for  $\delta = 2$  then  $M_D$  is at the order of  $\mathcal{O}(1 \text{ TeV})$ . An important consequence of large extra dimensions is the tower of Kaluza-Klein (KK) modes. Solutions of linear Einstein equations in  $4 + \delta$  dimension manifest themselves as a set of states separated in mass by  $\mathcal{O}(\frac{1}{R})$  in 4 dimension [47, 48]. In 4-dimensional effective theory we have spin-2 and spin-0 KK states that can interact with SM fields on the brane. Spin-2 and spin-0 states are sometimes called KK-gravitons and gravitational scalars respectively. KK-gravitons couple to the energy-momentum tensor of the SM fields. Although their coupling to SM fields is suppressed by a factor proportional to  $\frac{1}{M_{Pl}}$ , summation of enormous number of KK states in a tower provides an effective coupling of order  $\frac{1}{M_D}$ . Therefore, KK-gravitons can have observable effects at the TeV scale. Gravitational scalars is coupled only to the trace of the energy-momentum tensor. Since the trace of the energy-momentum tensor is zero for massless particles, the coupling of gravitational scalar to photons is zero at the tree-level. Hence, we will neglect gravitational scalars during amplitude calculations. Feynman rules for KK-gravitons were given in [47, 48].

The process  $\gamma q \rightarrow \gamma q$  is described by 3 tree-level diagrams (Fig.2). The polarization summed amplitude square can be written as

$$|M|^2 = |M_{SM}|^2 + |M_{KK}|^2 + |M_{int}|^2 \quad (2)$$

where  $M_{SM}$  is the SM amplitude,  $M_{KK}$  is the amplitude for the t-channel KK-graviton exchange and  $|M_{int}|^2$  represents interference terms between the SM and the KK amplitudes.

Analytical expressions for SM, KK and interference terms as a function of Mandelstam parameters  $\hat{s}$ ,  $\hat{t}$  and  $\hat{u}$  are

$$|M_{SM}|^2 = -8g_e^4 q^4 \left[ \frac{1}{(\hat{s} - m_q^2)^2} [3m_q^4 + \hat{s}\hat{u} - m_q^2(5\hat{s} + 2\hat{t} + 3\hat{u})] \right. \\ \left. + \frac{1}{(\hat{u} - m_q^2)^2} [3m_q^4 + \hat{s}\hat{u} - m_q^2(3\hat{s} + 2\hat{t} + 5\hat{u})] \right. \\ \left. - \frac{2}{(\hat{s} - m_q^2)(\hat{u} - m_q^2)} [6m_q^4 + 2m_q^2\hat{t} - m_q^2(\hat{s} + 4\hat{t} + \hat{u})] \right] \quad (3)$$

$$|M_{KK}|^2 = \frac{1}{2\bar{M}_{Pl}^4} |D(\hat{t})|^2 [(4m_q^2 - \hat{t})\hat{t} + (\hat{s} - \hat{u})^2] [2m_q^4 + \hat{s}^2 + \hat{u}^2 - 2m_q^2(\hat{s} - \hat{t} + \hat{u})] \quad (4)$$

$$|M_{int}|^2 = \frac{g_e^2 q^2 (D(\hat{t}) + D^*(\hat{t}))}{2\bar{M}_{Pl}^2} \left\{ \frac{1}{(\hat{s} - m_q^2)} [8m_q^6 - 2m_q^4(\hat{s} - 5\hat{t} + 7\hat{u}) \right. \\ \left. + (\hat{s} - \hat{t} - \hat{u})(3\hat{s}^2 + 2\hat{s}\hat{t} + \hat{t}^2 - (\hat{s} + \hat{t})\hat{u}) \right. \\ \left. + m_q^2(-3\hat{s}^2 + 10\hat{s}\hat{t} + \hat{t}^2 + 6\hat{s}\hat{u} - 2\hat{t}\hat{u} + 5\hat{u}^2)] \right. \\ \left. + (\hat{s} \longleftrightarrow \hat{u}) \right\} \quad (5)$$

where  $g_e = \sqrt{4\pi\alpha}$  and  $m_q$  is the mass of the quark.  $q$  is the quark charge which is given in units of positron charge. In eqs.(3-5) we do not write the factor due to initial spin average.  $\bar{M}_{Pl} = M_{Pl}/\sqrt{8\pi}$  is the reduced Planck mass.  $D(\hat{t})$  denotes propagator factors which are summed over infinite tower of KK modes. The existence of this infinite sum creates ultraviolet divergences even in tree-level processes. We employ the cutoff procedure that was assumed in Ref.[47] for phenomenological applications:

$$\frac{1}{\bar{M}_{Pl}^2} D(\hat{t}) = \frac{1}{\bar{M}_{Pl}^2} \sum_n \frac{1}{t - m_n^2} \equiv \frac{4\pi}{\Lambda_T^4} \quad \text{for } \delta > 2 \quad (6)$$

Here,  $\Lambda_T$  is an effective cutoff scale. Its dependence on  $M_D$  can be identified with some knowledge of the underlying quantum gravity theory. In case of string theory, the inequality  $M_D > \Lambda_T$  can be written [47]. As a consequence, any lower bound for  $\Lambda_T$  also serves as a lower bound for  $M_D$ .

The cross section for the main process  $pp \rightarrow p\gamma p \rightarrow p\gamma qX$  can be obtained by integrating the cross section for the subprocess  $\gamma q \rightarrow \gamma q$  over the photon and quark distributions:

$$\sigma(pp \rightarrow p\gamma p \rightarrow p\gamma qX) = \sum_q \int_{\xi_{min}}^{\xi_{max}} dx_1 \int_0^1 dx_2 \left( \frac{dN_\gamma}{dx_1} \right) \left( \frac{dN_q}{dx_2} \right) \hat{\sigma}_{\gamma q \rightarrow \gamma q}(\hat{s}) \quad (7)$$

where  $x_1$  is the fraction which represents the ratio between the scattered equivalent photon and initial proton energy and  $x_2$  is the momentum fraction of the proton's momentum carried by the struck quark.  $\frac{dN_\gamma}{dx_1}$  and  $\frac{dN_q}{dx_2}$  are the equivalent photon and quark distribution functions. Analytical expression for  $\frac{dN_\gamma}{dx_1}$  is given in the Appendix. Quark distribution functions have been evaluated numerically by using a code MSTW2008 [49]. The summation in (7) is performed over the following subprocesses:

$$\begin{aligned}
& \text{(i)} \quad \gamma u \rightarrow \gamma u & \text{(vi)} \quad \gamma \bar{u} \rightarrow \gamma \bar{u} \\
& \text{(ii)} \quad \gamma d \rightarrow \gamma d & \text{(vii)} \quad \gamma \bar{d} \rightarrow \gamma \bar{d} \\
& \text{(iii)} \quad \gamma c \rightarrow \gamma c & \text{(viii)} \quad \gamma \bar{c} \rightarrow \gamma \bar{c} \\
& \text{(iv)} \quad \gamma s \rightarrow \gamma s & \text{(ix)} \quad \gamma \bar{s} \rightarrow \gamma \bar{s} \\
& \text{(v)} \quad \gamma b \rightarrow \gamma b & \text{(x)} \quad \gamma \bar{b} \rightarrow \gamma \bar{b}
\end{aligned} \tag{8}$$

We estimate the sensitivity of the reaction  $pp \rightarrow p\gamma p \rightarrow p\gamma qX$  to extra dimensions using a simple one parameter  $\chi^2$  criterion without a systematic error. We have obtained 95% confidence level (C.L.) lower bounds for  $\Lambda_T$  considering forward detector acceptances of  $0.0015 < \xi < 0.15$ ,  $0.0015 < \xi < 0.5$ ,  $0.1 < \xi < 0.15$  and  $0.1 < \xi < 0.5$ . The first two are the AFP and CMS-TOTEM acceptances as we have mentioned in the introduction. The last two are the subintervals of the whole AFP and CMS-TOTEM acceptance regions. Forward detectors have a capability to detect intact protons in a continuous range of momentum fraction loss  $\xi$ . Hence, we can impose cuts and choose to work in a subinterval of the whole acceptance region. Since the KK terms in the amplitude square have a higher momentum dependence than the SM terms, imposing such cuts and removing low energy region of the whole acceptance range considerably suppress the SM contribution without minimizing the KK effects. During statistical analysis, the expected number of events is calculated through the formula:  $N = S \times E \times \sigma_{SM} \times L_{int}$ , where,  $L_{int}$  is the integrated luminosity,  $E$  is the jet reconstruction efficiency and  $S$  is the survival probability factor. We consider a survival probability factor of  $S = 0.7$  and jet reconstruction efficiency of  $E = 0.6$ . We have also imposed a pseudorapidity cut of  $|\eta| < 2.5$  for final (anti-)quarks and photons from subprocesses in (8).

In Fig.3 we present 95% C.L. lower bounds for  $\Lambda_T$  as a function of integrated LHC luminosity for AFP and CMS-TOTEM acceptances. The bounds have been obtained by considering three different virtualities  $Q^2 = M_Z^2, (5M_Z)^2$  and  $(10M_Z)^2$  for the deep inelastic

scattering where  $M_Z$  is the mass of the Z boson. In Fig.4 we present the lower bounds for  $0.1 < \xi < 0.15$  and  $0.1 < \xi < 0.5$  subintervals of the whole AFP and CMS-TOTEM acceptances. We see from these figures that the bounds for  $0.1 < \xi < 0.15$  and  $0.1 < \xi < 0.5$  cases are approximately 2 times stronger than the bounds for  $0.0015 < \xi < 0.15$  and  $0.0015 < \xi < 0.5$  respectively.

### III. RS MODEL OF WARPED EXTRA DIMENSIONS

Although the ADD model eliminate the hierarchy between the electroweak scale and the Planck scale, it introduces a new hierarchy between the electroweak scale and  $\frac{1}{R}$ . In this respect, RS model solves the hierarchy problem without generating an other large hierarchy. In the simplest RS model, we have only one extra spatial dimension and two branes located at orbifold fixed points  $y = 0$  and  $y = \pi r_c$  [4]. Here,  $y$  represents the extra dimensional coordinate and  $r_c$  is the compactification radius of the extra dimension. The brane which is located at  $y = \pi r_c$  is called the TeV-brane where SM fields live on. The brane at  $y = 0$  is called the Planck-brane. As in the case of ADD model, gravity can propagate to everywhere. TeV and Planck branes have different vacuum energies and the 5 dimensional bulk bounded by these branes has a cosmological constant  $\Lambda$ . Assuming four dimensional Poincare invariance, the solution to Einstein's field equations is given by the following metric [4]:

$$ds^2 = e^{-2k|y|} \eta_{\mu\nu} dx^\mu dx^\nu - dy^2, \quad (9)$$

where  $k$  is a constant of order the Planck scale. It is also deduced from the solution of Einstein's field equations that TeV and Planck branes have equal magnitude but opposite sign tensions and  $\Lambda < 0$ . Therefore, the spacetime in between TeV and Planck branes is a slice of an  $AdS_5$  geometry. Inserting metric (9) into the action for the gravity and integrating over extra dimensional coordinate  $y$ , we obtain the following relation between the Planck scale and the fundamental scale:

$$\bar{M}_{Pl}^2 = \frac{M^3}{k} (1 - e^{-2kr_c\pi}). \quad (10)$$

If  $k \sim \bar{M}_{Pl}$  and  $e^{-2kr_c\pi}$  is very small then the hierarchy between  $\bar{M}_{Pl}$  and  $M$  is eliminated. From the action for matter fields we can deduce that any mass scale  $m_0$  on the TeV brane

in the higher dimensional theory will correspond to a physical mass  $e^{-kr_c\pi}m_0$ . The factor  $e^{-kr_c\pi}$  is called warp factor. If  $kr_c \sim 12$  then the warp factor is small enough to generate TeV scale masses from the masses of order  $M_{Pl}$ . Hence, RS model solves the hierarchy problem without generating a large hierarchy between  $k$  and  $\frac{1}{r_c}$ .

In the RS model, KK graviton mass spacing is quite large compared with the ADD model. The mass spectrum is given by  $m_n = x_n k e^{-kr_c\pi} = x_n \beta \Lambda_\pi$  where  $\beta = k/\bar{M}_{Pl}$  and  $x_n$  are the roots of  $J_1(x_n) = 0$  [50]. Therefore the mass spacing is at the order of TeV scale. Summation in the graviton propagator can not be approximated to an integral. Instead, discrete graviton mass spectrum should be considered in the summation. Since the contribution of the KK graviton excitations to the propagator is small for masses above the center-of-mass energy of the process, we can cut off the series at some finite mass value. During calculations, we have considered first four roots of the Bessel function. Another important feature of the RS model is that massive KK graviton excitations couple to SM fields with a coupling constant  $\frac{1}{\Lambda_\pi}$  where  $\Lambda_\pi$  is a scale of the order of TeV.

Amplitude square for the process  $\gamma q \rightarrow \gamma q$  in the RS model can be easily obtained from (4) and (5) through the replacement [50]:

$$\frac{1}{\bar{M}_{Pl}^2} D(\hat{t}) \longrightarrow \frac{1}{2\Lambda_\pi^2} \sum_n \frac{1}{\hat{t} - m_n^2 + im_n \Gamma_n} \quad (11)$$

where the decay width for the nth KK graviton excitation is  $\Gamma_n = \rho m_n (\frac{m_n}{\Lambda_\pi})^2$ . Here,  $\rho$  is a constant which is assumed to be 1.

We have obtained 95% C.L. excluded regions in the  $\beta - m_G$  plane using a similar statistical analysis that was performed for the ADD model. Here,  $m_G$  is the mass of the first KK graviton excitation, i.e.,  $m_G = m_1$ . We present our results in Fig.5 for two different forward detector acceptances  $0.1 < \xi < 0.15$  and  $0.1 < \xi < 0.5$ . The limits for the whole AFP and CMS-TOTEM acceptance regions are weaker than the limits for  $0.1 < \xi < 0.15$  and  $0.1 < \xi < 0.5$  subintervals. Hence, we do not present them.

#### IV. CONCLUSIONS

We have investigated the potential of  $pp \rightarrow p\gamma p \rightarrow p\gamma q X$  reaction at the LHC to probe large and warped extra dimensions. The bounds that we have obtained for the ADD model are better than the bounds obtained in photon-induced reactions  $pp \rightarrow p\gamma\gamma p \rightarrow p\ell^+\ell^-p$  [27],



$pp \rightarrow p\gamma\gamma p \rightarrow p\gamma\gamma p$  [32] and  $pp \rightarrow p\gamma\gamma p \rightarrow p\bar{t}t p$  [39] at the LHC. Recent results on large extra dimensions from CMS and ATLAS experiments provide stringent limits [51–56]. Our limits on  $\Lambda_T$  for an acceptance of  $0.1 < \xi < 0.5$  are better than these current experimental bounds. In the case of RS model, excluded region of the model parameters extends to wider regions than the case of the reaction  $pp \rightarrow p\gamma\gamma p \rightarrow p\ell^+\ell^-p$  [27] and is comparable to the case of the reaction  $pp \rightarrow p\gamma\gamma p \rightarrow p\gamma\gamma p$  [32]. However, our limits on RS model parameters are weaker than the recent experimental bounds [56]. Therefore the reaction  $pp \rightarrow p\gamma p \rightarrow p\gamma q X$  has a considerable potential in probing large extra dimensions of the ADD model. On the other hand, this is not the case for the RS model.

### Acknowledgments

This work has been supported by the Scientific and Technological Research Council of Turkey (TÜBİTAK) in the framework of the project no: 112T085.

### Appendix: Equivalent photon approximation and photon spectrum

Incoming photon beam in the subprocess  $\gamma q \rightarrow \gamma q$  is described by EPA. According to EPA, equivalent photon distribution for photons which are emitted from a proton beam is given through the formula [8–10]:

$$\frac{dN_\gamma}{dE_\gamma dQ^2} = \frac{\alpha}{\pi} \frac{1}{E_\gamma Q^2} \left[ \left(1 - \frac{E_\gamma}{E}\right) \left(1 - \frac{Q_{min}^2}{Q^2}\right) F_E + \frac{E_\gamma^2}{2E^2} F_M \right] \quad (\text{A.1})$$

where

$$Q_{min}^2 = \frac{m_p^2 E_\gamma^2}{E(E - E_\gamma)}, \quad F_E = \frac{4m_p^2 G_E^2 + Q^2 G_M^2}{4m_p^2 + Q^2} \quad (\text{A.2})$$

$$G_E^2 = \frac{G_M^2}{\mu_p^2} = \left(1 + \frac{Q^2}{Q_0^2}\right)^{-4}, \quad F_M = G_M^2, \quad Q_0^2 = 0.71 \text{ GeV}^2 \quad (\text{A.3})$$

In the above formula,  $Q^2$  and  $E_\gamma$  are the virtuality and energy of the photon spectrum.  $E$  is the energy of the incoming proton beam.  $m_p$  and  $\mu_p$  denote the mass and the magnetic moment of the proton.  $F_E$  and  $F_M$  are functions of the electric and magnetic form factors. After integration over  $dQ^2$  in the interval  $Q_{min}^2 - Q_{max}^2$ , equivalent photon distribution can be written as [14]

$$\frac{dN_\gamma}{dE_\gamma} = \frac{\alpha}{\pi E_\gamma} \left(1 - \frac{E_\gamma}{E}\right) \left[ \varphi\left(\frac{Q_{max}^2}{Q_0^2}\right) - \varphi\left(\frac{Q_{min}^2}{Q_0^2}\right) \right]. \quad (\text{A.4})$$

Here, the function  $\varphi$  is defined by

$$\begin{aligned} \varphi(x) = (1 + ay) & \left[ -\ln\left(1 + \frac{1}{x}\right) + \sum_{k=1}^3 \frac{1}{k(1+x)^k} \right] + \frac{y(1-b)}{4x(1+x)^3} \\ & + c \left(1 + \frac{y}{4}\right) \left[ \ln\left(\frac{1-b+x}{1+x}\right) + \sum_{k=1}^3 \frac{b^k}{k(1+x)^k} \right] \end{aligned} \quad (\text{A.5})$$

where

$$\begin{aligned} y &= \frac{E_\gamma^2}{E(E - E_\gamma)}, \quad a = \frac{1 + \mu_p^2}{4} + \frac{4m_p^2}{Q_0^2} \approx 7.16 \\ b &= 1 - \frac{4m_p^2}{Q_0^2} \approx -3.96, \quad c = \frac{\mu_p^2 - 1}{b^4} \approx 0.028 \end{aligned} \quad (\text{A.6})$$

The contribution to the integral above  $Q_{max}^2 \approx 2 \text{ GeV}^2$  is negligible. Therefore during calculations we set  $Q_{max}^2 = 2 \text{ GeV}^2$ .

- 
- [1] N. Arkani-Hamed, S. Dimopoulos and G. R. Dvali, Phys. Lett. B **429**, 263 (1998) [hep-ph/9803315].
  - [2] N. Arkani-Hamed, S. Dimopoulos and G. R. Dvali, Phys. Rev. D **59**, 086004 (1999) [hep-ph/9807344].
  - [3] I. Antoniadis, N. Arkani-Hamed, S. Dimopoulos and G. R. Dvali, Phys. Lett. B **436**, 257 (1998) [hep-ph/9804398].
  - [4] L. Randall and R. Sundrum, Phys. Rev. Lett. **83**, 3370 (1999) [hep-ph/9905221].
  - [5] X. Rouby, Ph.D. thesis, Universite Catholique de Louvain [UCL-Thesis 135-2008 and CMS TS-2009/004, 2008].
  - [6] J. de Favereau de Jeneret, V. Lemaitre, Y. Liu, S. Oryn, T. Pierzchala, K. Piotrkowski, X. Rouby, N. Schul and M. Vander Donckt, arXiv:0908.2020 [hep-ph].
  - [7] N. Schul, Ph.D. thesis, Universite Catholique de Louvain [CERN-THESIS-2011-271 and CMS-TS-2011-030].
  - [8] V. M. Budnev, I. F. Ginzburg, G. V. Meledin and V. G. Serbo, Phys. Rep. **15**, 181 (1975).
  - [9] G. Baur *et al.*, Phys. Rep. **364**, 359 (2002).
  - [10] K. Piotrkowski, Phys. Rev. D **63**, 071502 (2001) [hep-ex/0009065].
  - [11] C. Royon *et al.* (RP220 Collaboration), arXiv:0706.1796 [physics.ins-det], *Proceedings for the DIS 2007 workshop, Munich, 2007*.

- [12] M.G. Albrow *et al.* (FP420 R and D Collaboration), J. Instrum. **4**, T10001 (2009); arXiv:0806.0302 [hep-ex].
- [13] V. Avati and K. Osterberg, Report No. CERN-TOTEM-NOTE-2005-002, 2006.
- [14] O. Kepka and C. Royon, Phys. Rev. D **78**, 073005 (2008); arXiv:0808.0322 [hep-ph].
- [15] A. Abulencia *et al.* (CDF Collaboration), Phys. Rev. Lett. **98**, 112001 (2007); arXiv:hep-ex/0611040.
- [16] T. Aaltonen *et al.* (CDF Collaboration), Phys. Rev. Lett. **102**, 222002 (2009); arXiv:0902.2816 [hep-ex].
- [17] T. Aaltonen *et al.* (CDF Collaboration), Phys. Rev. Lett. **102**, 242001 (2009); arXiv:0902.1271 [hep-ex].
- [18] S. Chatrchyan *et al.* [CMS Collaboration], JHEP **1201**, 052 (2012) [arXiv:1111.5536 [hep-ex]].
- [19] S. Chatrchyan *et al.* [CMS Collaboration], JHEP **1211**, 080 (2012) [arXiv:1209.1666 [hep-ex]].
- [20] I. F. Ginzburg and A. Schiller, Phys. Rev. D **57**, 6599 (1998) [hep-ph/9802310].
- [21] I. F. Ginzburg and A. Schiller, Phys. Rev. D **60**, 075016 (1999) [hep-ph/9903314].
- [22] V.A. Khoze, A.D. Martin and M.G. Ryskin, Eur. Phys. J. C **23**, 311 (2002); arXiv:hep-ph/0111078.
- [23] N. Schul and K. Piotrkowski, Nucl. Phys. B, Proc. Suppl., **179**, 289 (2008); arXiv:0806.1097 [hep-ph].
- [24] S. M. Lietti, A. A. Natale, C. G. Roldao and R. Rosenfeld, Phys. Lett. B **497**, 243 (2001); arXiv:hep-ph/0009289.
- [25] T. Pierzchala and K. Piotrkowski, Nucl. Phys. Proc. Suppl. **179-180**, 257 (2008); arXiv:0807.1121 [hep-ph].
- [26] E. Chapon, C. Royon and O. Kepka, Phys. Rev. D **81**, 074003 (2010); arXiv:0912.5161 [hep-ph].
- [27] S. Atağ, S. C. İnan and İ. Şahin, Phys. Rev. D **80**, 075009 (2009); arXiv:0904.2687 [hep-ph].
- [28] İ. Şahin and S. C. İnan, JHEP **09**, 069 (2009); arXiv:0907.3290 [hep-ph].
- [29] T. Dougall and S. D. Wick, Eur. Phys. J. A **39**, 213 (2009) [arXiv:0706.1042 [hep-ph]].
- [30] M. Chaichian, P. Hoyer, K. Huitu, V. A. Khoze and A. D. Pilkington, JHEP **0905**, 011 (2009) [arXiv:0901.3746 [hep-ph]].
- [31] K. Piotrkowski and N. Schul, AIP Conf. Proc. **1200**, 434 (2010) [arXiv:0910.0202 [hep-ph]].
- [32] S. Atağ, S. C. İnan and İ. Şahin, JHEP **09**, 042 (2010); arXiv:1005.4792 [hep-ph].

- [33] V. P. Goncalves and W. K. Sauter, Phys. Rev. D **82**, 056009 (2010) [arXiv:1007.5487 [hep-ph]].
- [34] S. C. İnan, Phys. Rev. D **81**, 115002 (2010); arXiv:1005.3432 [hep-ph].
- [35] S. Atağ and A. A. Billur, JHEP **11**, 060 (2010); arXiv:1005.2841 [hep-ph].
- [36] M.G. Albrow, T.D. Coughlin and J.R. Forshaw, Prog. Part. Nucl. Phys. **65**, 149-184 (2010); arXiv:1006.1289 [hep-ph].
- [37] İ. Şahin, and A. A. Billur, Phys. Rev. D **83**, 035011 (2011); arXiv:1101.4998 [hep-ph].
- [38] İ. Şahin, and M. Koksas, JHEP **03**, 100 (2011); arXiv:1010.3434 [hep-ph].
- [39] S. C. Inan and A. A. Billur, Phys. Rev. D **84**, 095002 (2011).
- [40] R. S. Gupta, Phys. Rev. D **85**, 014006 (2012) [arXiv:1111.3354 [hep-ph]].
- [41] İ. Şahin, Phys. Rev. D **85**, 033002 (2012) [arXiv:1201.4364 [hep-ph]].
- [42] L. N. Epele, H. Fanchiotti, C. A. G. Canal, V. A. Mitsou and V. Vento, Eur. Phys. J. Plus **127**, 60 (2012) [arXiv:1205.6120 [hep-ph]].
- [43] B. Şahin and A. A. Billur, Phys. Rev. D **86**, 074026 (2012) [arXiv:1210.3235 [hep-ph]].
- [44] İ. Şahin and B. Şahin, Phys. Rev. D **86**, 115001 (2012) [arXiv:1211.3100 [hep-ph]].
- [45] A. A. Billur, Europhys. Lett. **101**, 21001 (2013).
- [46] A. Senol, Phys. Rev. D **87**, 073003 (2013) [arXiv:1301.6914 [hep-ph]].
- [47] G. F. Giudice, R. Rattazzi and J. D. Wells, Nucl. Phys. B **544**, 3 (1999) [hep-ph/9811291].
- [48] T. Han, J. D. Lykken and R. -J. Zhang, Phys. Rev. D **59**, 105006 (1999) [hep-ph/9811350].
- [49] A. D. Martin, W. J. Stirling, R. S. Thorne and G. Watt, Eur. Phys. J. C **63**, 189 (2009) [arXiv:0901.0002 [hep-ph]].
- [50] H. Davoudiasl, J. L. Hewett and T. G. Rizzo, Phys. Rev. Lett. **84**, 2080 (2000) [hep-ph/9909255].
- [51] M. Marionneau [on behalf of the ATLAS and CMS Collaboration], arXiv:1305.3169 [hep-ex].
- [52] ATLAS Collaboration, ATLAS-CONF-2012-147.
- [53] CMS Collaboration, CMS-PAS-EXO-12-027.
- [54] CMS Collaboration, CMS-PAS-EXO-12-031.
- [55] G. Aad *et al.* [ATLAS Collaboration], Phys. Rev. D **87**, 015010 (2013) [arXiv:1211.1150 [hep-ex]].
- [56] G. Aad *et al.* [ATLAS Collaboration], New J. Phys. **15**, 043007 (2013) [arXiv:1210.8389 [hep-ex]].

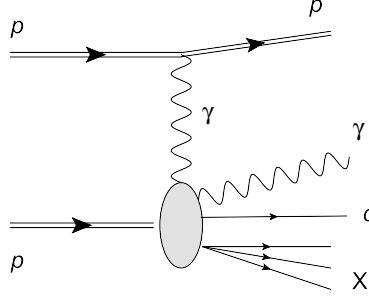


FIG. 1: Schematic diagram for the reaction  $pp \rightarrow p\gamma p \rightarrow p\gamma q X$ .

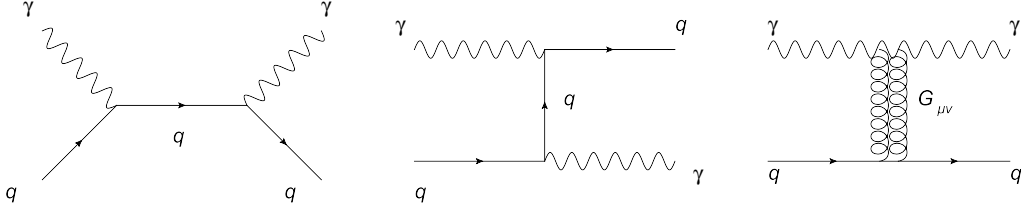


FIG. 2: Tree-level Feynman diagrams for the subprocess  $\gamma q \rightarrow \gamma q$  ( $q = u, d, c, s, b, \bar{u}, \bar{d}, \bar{c}, \bar{s}, \bar{b}$ ) in the presence of Kaluza-Klein graviton mediation.

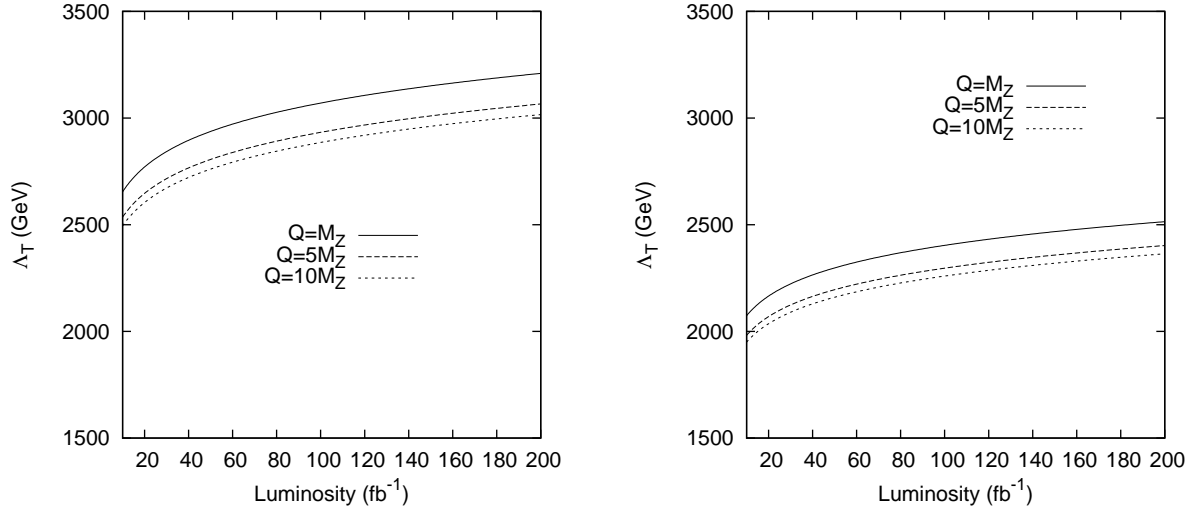


FIG. 3: 95% C.L. lower bounds for  $\Lambda_T$  as a function of integrated LHC luminosity for forward detector acceptance regions  $0.0015 < \xi < 0.5$  (left panel) and  $0.0015 < \xi < 0.15$  (right panel). Legends are for various values of the virtuality of the deep inelastic scattering.

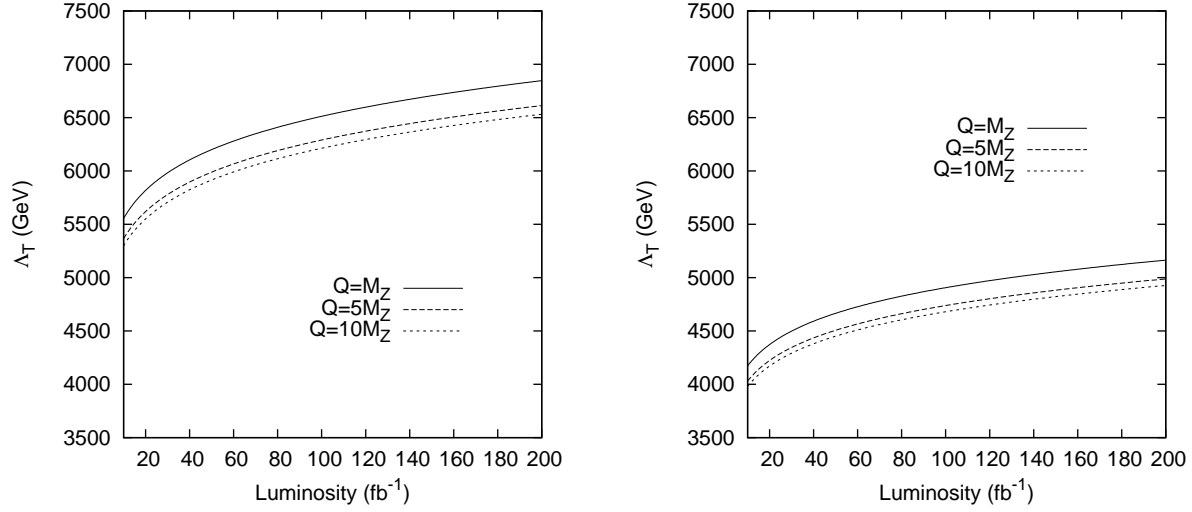


FIG. 4: 95% C.L. lower bounds for  $\Lambda_T$  as a function of integrated LHC luminosity for forward detector acceptance regions  $0.1 < \xi < 0.5$  (left panel) and  $0.1 < \xi < 0.15$  (right panel). Legends are for various values of the virtuality of the deep inelastic scattering.

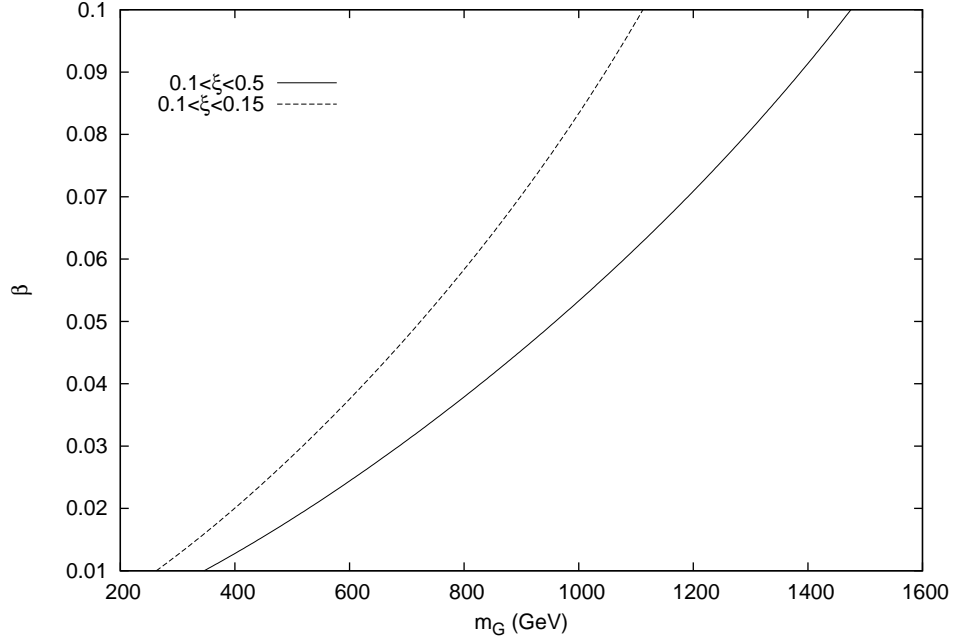


FIG. 5: Limits in the  $\beta - m_G$  plane for an integrated luminosity of  $200 \text{ fb}^{-1}$ . The regions above the curves are excluded at 95% C.L. The virtuality of the deep inelastic scattering is taken to be  $Q^2 = (5M_Z)^2$  where  $M_Z$  is the mass of the Z boson.